Δελτίο της Ελληνικής Γεωλογικής Εταιρίας, τομ. XLVII , 2013
Πρακτικά 13ου Διεθνούς Συνεδρίου, Χανιά, Σεπτ. 2013

Bulletin of the Geological Society of Greece, vol. XLVII 2013
Proceedings of the 13th International Congress, Chania, Sept. 2013

THE 1912 GANOS EARTHQUAKE: SOURCE CONSTRAINTS USING GROUND MOTION SIMULATIONS

Kiratzi A.

Department of Geophysics, Aristotle University of Thessaloniki, Greece (Kiratzi@geo.auth.gr)

Abstract

We study the source characteristics of the 9 August 1912, Mw 7.4, Mürefte (Ganos) earthquake that ruptured the Ganos Fault in the westernmost segment of the North Anatolian Fault. We apply the stochastic method for finite-faults in order to simulate strong ground motion acceleration using different fault geometries in terms of the rupture initiation and the length of the fault. A first-order approximation of the site effect variation is achieved following an empirical approach based on the topography gradient as a proxy for site-effect. The simulated ground motions, which are calculated at phantom stations, over a grid covering the area of study, satisfactorily produce the regions which were more severely shaken during the 1912 event. We simulate ground motions using a conservative fault length of 50 km (one land segment) which is able to explain the location of the surface ruptures but is not able to reproduce the surface extent of strong shaking. We then use a longer fault of approximately 120 km, extending to Saros Bay in the west and to Marmara Sea in the east. The synthetic peak ground acceleration values, indicate a segmented nature of the fault, have at least two patches of strong shaking and significantly predict the observed macroseismic intensities of the 1912 earthquake. Further constrain in our modelling is posed by surface ruptures, with small releasing and restraining structures and 1.5–5.5 m right-lateral offsets, that have been previously measured by others, at 45 sites of the on-land ~50-km-long fault section.
Key words: *Ganos fault; North Anatolian fault; Mürefte; deformation.*

Περίληψη

Ο σημαντικότερος σεισμός στο δυτικό άκρο του ρήγματος της Β. Ανατόλιας είναι αυτός της 9ης Αυγούστου 1912, Mw 7.4. Για τη μελέτη των χαρακτηριστικών της πηγής, και ειδικότερα του μήκους του ρήγματος που τον προκάλεσε καθώς και του σημείου έναρξης και διάδοσης της διάρρηξης, γίνεται στοχαστική προσομοίωση των εδαφικών κινήσεων. Στους κόμβους ενός πλέγματος που καλύπτει την ευρύτερη περιοχή υπολογίζεται η μέγιστη εδαφική επιτάχυνση από δυο σενάρια: κατά το πρώτο σενάριο το μήκος του ρήγματος είναι μόνο 50 km, όπως η επιφανειακή εμφάνιση στην ξηρά. Οι τιμές της επιτάχυνσης, διορθωμένες και για τις εδαφικές συνθήκες, αποτυπώνουν τις περιοχές στην ξηρά με τις μέγιστες μετρήσεις ολίσθησης, αλλά η συνολική επιφάνεια μέγιστης παραμόρφωσης είναι μικρότερη από την παρατηρηθείσα. Καλύτερη αποτύπωση γίνεται για ένα ρήγμα μήκους 1200 km, το οποίο πέρα από την ξηρά εκτείνεται τόσο στη θάλασσα του Μαρμαρά στα ανατολικά, όσο και στον Κόλπο του Σάρου στα δυτικά. Οι μέγιστες εδαφικές επιταχύνσεις αποτυπώνουν τουλάχιστον δυο περιοχές με ισχυρές εδαφικές κινήσεις, το οποίο μπορεί να εκληφθεί και ως

ένδειξη πολλαπλών πηγών κατά τη διάρρηξη. Για την αξιολόγηση των αποτελεσμάτων των στοχαστικών προσομοιώσεων συνεκτιμήθηκαν και οι μετρήσεις της επιφανειακής ολίσθησης κατά μήκος του ρήγματος
Λέξεις κλειδιά: *Μυριόφυτο, ρήγμα Ganos, παραμόρφωση, Ρήγμα Βόρειας Ανατόλιας.*

1. Introduction

The most significant earthquake at the western end of the North Anatolian Fault Zone (Figure 1), along the Ganos Fault Zone (GFZ) is the 9 August 1912 event (40.7°N, 27.2°E; UTC 01:29; Ms 7.0 to 7.6; Mw7.4) also known as Sarköy-Mürefte or Saros-Marmara earthquake (Ambraseys and Jackson, 1998, 2000; Janssen et al., 2009). The Ganos Fault Zone extends from the Tekirdag Basin in the east, up to the Island of Samothrace in the west, passing through the town of Gaziköy and the Saros Trough (Armijo et al., 1999; Seeber et al., 2004; Karabulut et al., 2006).

The earthquake caused the loss of 2,836 people, while more than 7,000 were injured. More than 300 villages suffered damage (Altinok et al., 2003; Papazachos and Papazachou, 2003), mainly to the north of Dardanelles. Liquefaction was observed to distances up to 180 km from the epicentre, indicating the level of strong ground motions. Long period ground motions were responsible for serious damage to public buildings as far as Edirne to the north and Istanbul to the east of the epicentre, The mainshock was followed by many aftershocks; the strongest was the one that occurred within hours after the mainshock (UTC 09:23; Ms 6.2). On 13 September 1912 (UTC 23:32) a second shock occurred of Ms 6.7 (Mw6.8), with an epicentre (40.1°N, 26.8°E) located at the westernmost edge of the August mainshock rupture, and was considered as a triggered event (Papadimitriou et al., 2001).

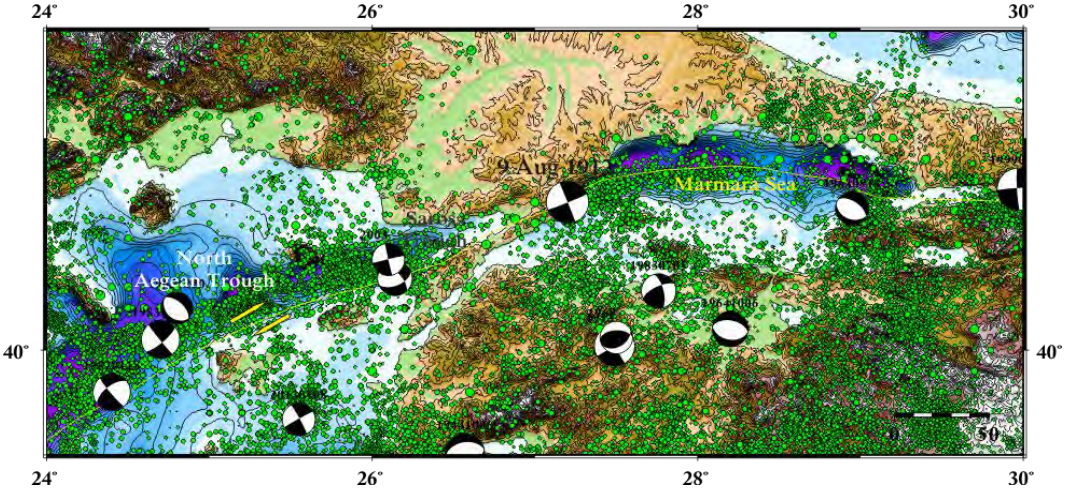

Figure 1 - The location of the 9 August 1912 earthquake along the Ganos Fault Zone. The beach- balls (from Kiratzi and Louvari, 2003; Kiratzi et al., 2007) denote the available focal mechanisms for previous events with Mw>6.0. The seismicity of the period 550BC- 2012 with M>5.0 is also plotted (green circles).

The 1912 earthquake has attracted the attention of many scientists mainly because it is connected with the inferred sub-marine fault system to the Marmara Sea, which poses a constant threat to the metropolitan city of Istanbul. Moreover, the connection of the Ganos Fault with other fault segments capable to produce strong earthquakes makes it even more significant.

The Ganos Fault Zone (GFZ) joins the northern strand of the North Anatolian Fault Zone (NAFZ) in the Marmara Sea and the North Aegean Sea. The western continuation of the NAFZ into the

North Aegean Trough is portioned and two main branches can be identified. The GFZ is clearly visible on satellite images. The northern part of the zone is bounded by the Ganos Mountains, which are considered to develop during the end of Miocene due to an episode of transpressional uplift, resulting from right lateral strike-slip motion, which in total is ~40 km.

The total rupture length of the 1912 earthquake is a matter of dispute. Most people agree that the length is well above the 50 km land segment, but what is the extent of the rupture into the Saros Trough and what is its extent into the western Marmara Sea is again controversial. For example, the rupture length is considered between 90 to 150 km (Aksoy et al., 2010 and references therein). The purpose of the present study is to examine a number of locations of the rupture initiation and two fault lengths in order to test their capability to reproduce the gross characteristics of the measured surface slip along-strike of the fault and to the distribution of damage (Figure 2) in the most affected region (Ambraseys and Finkel, 1987). To do so, stochastic ground simulations are performed using the method of Boore (1983) as used by Beresnev and Atkinson (1997, 1998).

2. Observations for Ground Motion Validation

The 9 August 1912 mainshock produced a surface expression of the fault with a distinct right lateral strike-slip motion (see Table 1 for parameters). The measured length on land was 45 - 50 km (Ambraseys and Finkel, 1987; Altunel et al., 2004). The long-period records from a small number of Wiechert seismographs were used to estimate the magnitude of this earthquake (Ambraseys and Jackson, 1998; Aksoy et al., 2010). The large magnitude ($M_w = 7.4$), declares that complimentary to the ~50 km land segment co-seismic faulting must have extended off-shore, towards the south-west into the Gulf of Saros, and towards the north-east into the Marmara Sea near Güzelkoy.

Table 1 – Information on the focal mechanism solutions reported for the 1912 shocks.

Date Y/MM/DD	Origin Time hh:mm	Lat	Long	Mw	NODAL PLANE 1 Strike° Dip° Rake°			NODAL PLANE 2 Strike° Dip° Rake°			Ref
19120809	01:29	40.7	27.2	7.3	41	60	-135	284	52	-39	1
#	#	40.7	27.2	7.4	68	88	180	158	89	2	2
19120809	09:23	40.8	27.5	6.2							1
19120913	23:32	40.7	27.0	6.8							1

References 1: Jackson and McKenzie 1988; 2: Aksoy et al., 2010

The distribution of the isoseismals for the 1912 mainshock clearly shows that in the mezoseismal region intensities were of the order of IX (Figure 2). The length of the major-axis of the contour of intensity IX is about 110 km. Complimentary to the distribution of observed intensities, there are data from the slip measured at 45 sites, along the land segment of the fault (Aksoy et al., 2010). These slip values range from 1.4 meters to 5.5 meters, with a median value of 4 m (Figure 3). The average slip is of the order of 2.5 m.

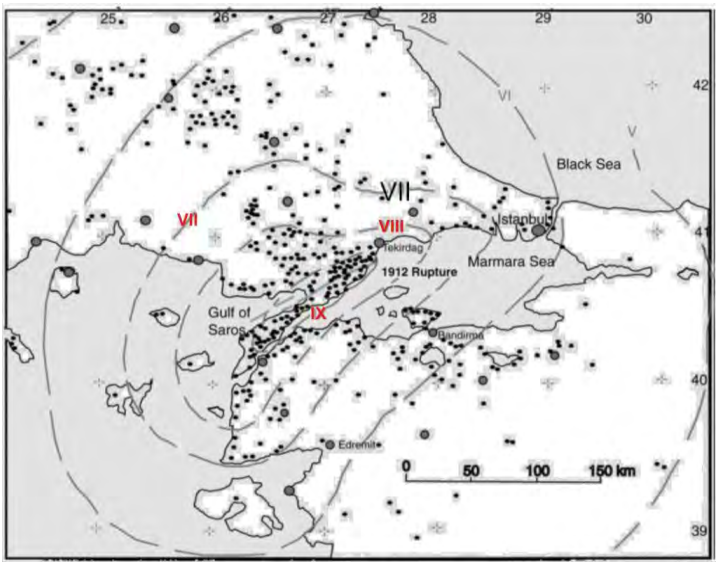

Figure 2 - Isoseismal map for the 1912 mainshock (from Ambraseys and Finkel, 1987). Note the distribution of intensity IX, which roughly has a length of ~110 km.

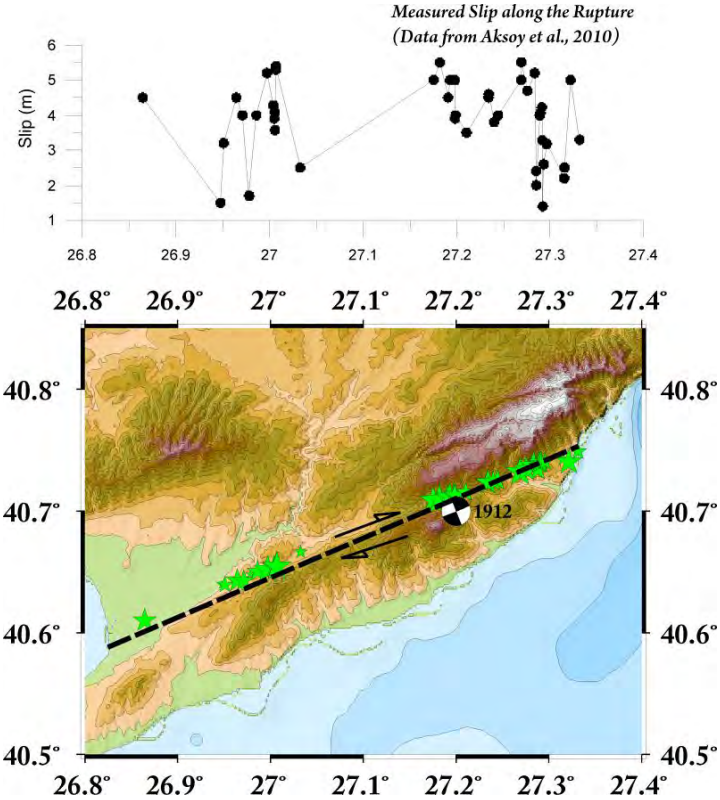

Figure 3 - Measured surface slip for the 1912 Ganos earthquake (top) as given by Aksoy et al., 2010, to compare with the assumed land fault segment and the assumed epicentre location, given by the beach-ball (bottom). Green asterisks denote the points where slip was measured.

3. Strong Ground Motion Modelling

3.1 Method

The core of the method used relies on the observation that a considerable portion of the strong ground motion, mainly related to the onset of S-waves, can be approximated as white noise. In parallel, the Fourier Amplitude Spectrum of a Brune omega-squared type source is stable and independent of frequency, for the frequencies between the corner frequency, fc and fmax. This led to the hypothesis that the strong ground motion, between the frequencies of fc and fmax, can be approximated by white noise.

The applied method requires a simple representation of all factors affecting strong ground motion. The source is approximated by a rectangular fault, and the propagation parameters (geometric spreading, inelastic attenuation, near-surface attenuation and site amplification) are described by empirical relations and factors. As mentioned, the method involves discretization of the fault plane into a number of sub-faults, each of which is assigned an ω^{-2} spectrum. Contributions from all sub-faults are empirically attenuated to the observation site using $Q(f) = 50f^{1.09}$ (Pulido et al., 2004) and appropriately summed to produce the synthetic accelerograms. Near-surface attenuation of the seismic waves was modelled using the kappa, κ, operator and diminishing the simulated spectra by $exp(-\pi\kappa f)$. Simulations at all sites of interest were performed assuming rock site conditions at the ground surface.

A first-order incorporation of the site effect in the computed ground motion parameters was based on the work of Wald and Allen (2007). They correlate the topography gradient of a region with VS_{30} (average shear-wave velocity at the top 30 meters of the soil column), which are often used as a proxy for soil characterization. Based on the VS_{30} value and the amplitude of the peak ground acceleration in the synthetic accelerograms at the specific grid point an appropriate empirical amplification factor for the PGA (Borcherdt, 1994) was selected.

3.2 Case 1: Conservative Fault Length

In this case the total along-strike length of the fault is taken equal to 50 km; the fault is placed on its surface expression on the land (Figure 3). The width of the fault is taken to be 17 km. The number of sub-faults along strike and along dip is 9 and 3, respectively. The purpose of the simulation is to see what the land segment of the rupture, can reproduce. The fault strike is taken as 68°, the dip is taken equal to 88° (Aksoy et al., 2010; see Table1).

The rupture starts from sub-fault [9, 3] that is at the easternmost and deepest location of the fault and propagates towards west. This rupture initiation point was chosen after a number of trial runs, and was found to reproduce better the observed surface deformation. The simulations were performed over a grid covering the broader region and spaced at 0.05°. At each grid point a simulated horizontal component of shear wave from the finite fault was computed.

Figure 4 summarizes the simulations results. To produce this figure the simulated accelerations at each grid point, were corrected first for the site – effect and then they were converted to intensities in order to compare the predicted values within the mezoseismal area with those reported by Ambraseys and Finkel (1987).

A conservative fault length that aligns along the observed surface expression of the rupture is capable to reproduce the level of damage at the mezoseismal region. For example the simulated intensities are of the order of 8.5 to 9, as in the observed intensities (Figure 2). The area covered though by isoseismal IX though, is considerably smaller compared to the regional extent of IX in the case of observed damage.

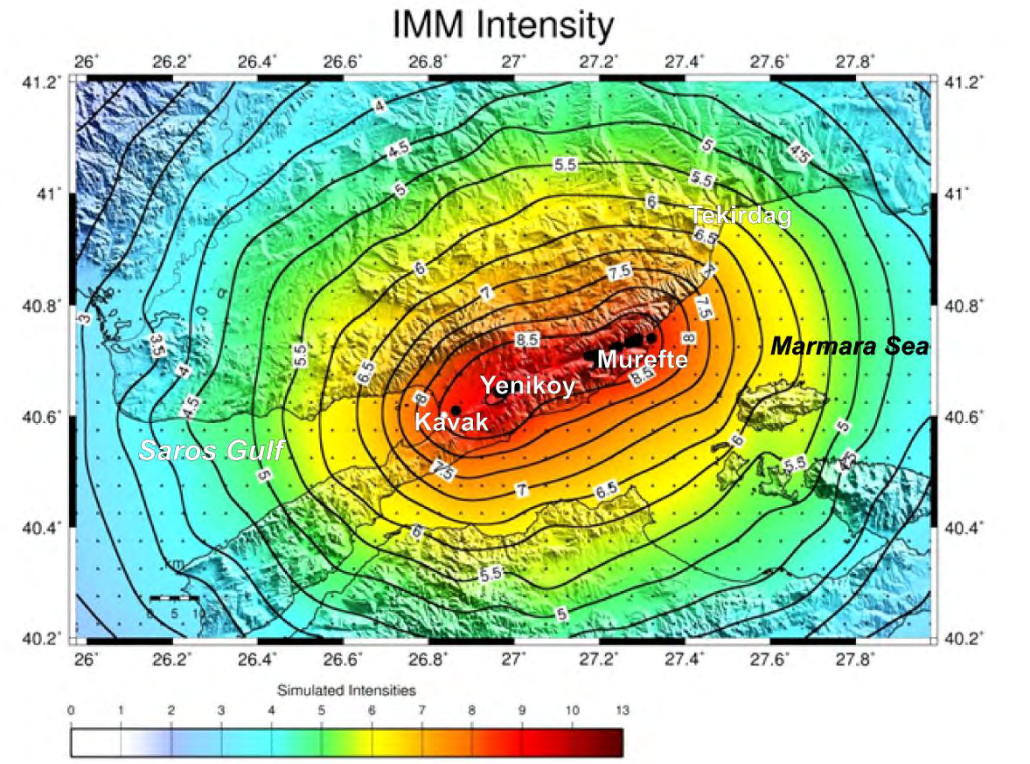

Figure 4 - Simulated distribution of intensities for the 1912 Ganos earthquake, using a finite fault with length equal to 50 km. The fault location is placed along the land expression of the rupture. The model predicts intensities 8 to 9 in the mezoseismal area, but of considerable smaller area, compared to the area observed (see Figure 2). The points where surface slip exceeded 4 m are marked as black dots. The white dot marks the western edge of the model finite-fault which extents 50 km to the east.

3.3 Case 2: Large Fault Length

The next step was to imply the largest length for the causative fault and to examine the percentage of the length extent in the west (e.g. Saros Gulf) as well as the length required at the eastern end, at the Marmara Sea. A number of fault lengths and end-member extents were tested and finally the value adopted was for a 120 km length fault of 18 km width along dip, in agreement with empirical scaling relations (Wells and Coppersmith, 1994). The same focal mechanism was used in this case, also. In this simulation the fault was discretized in 24×3 sub-faults, along strike and along dip, respectively. The rupture initiated at sub-fault (14, 3) using the local coordinates, which is at the deepest point of the fault and close to the epicentre.

More specifically for this fault length the length of the rupture into the Saros Bay was 40 km, 50 km on land and 30 km into the Marmara Sea. The simulated ground motions are presented in Figure 5. The map represents the distribution of simulated PGA's at the broader region, and it is observed that the simulations predict two patches of strong shaking: one extending east of the adopted hypocenter and into the Marmara Sea, with the strongest shaking observed ~25 km east of Tekirdag. The second patch of strong shaking is extending to the west of the hypocenter and its shape is two-lobe. One lobe is observed near Kavak while the other is further to the west, at the opening of the Saros Bay, north of Yeniköy.

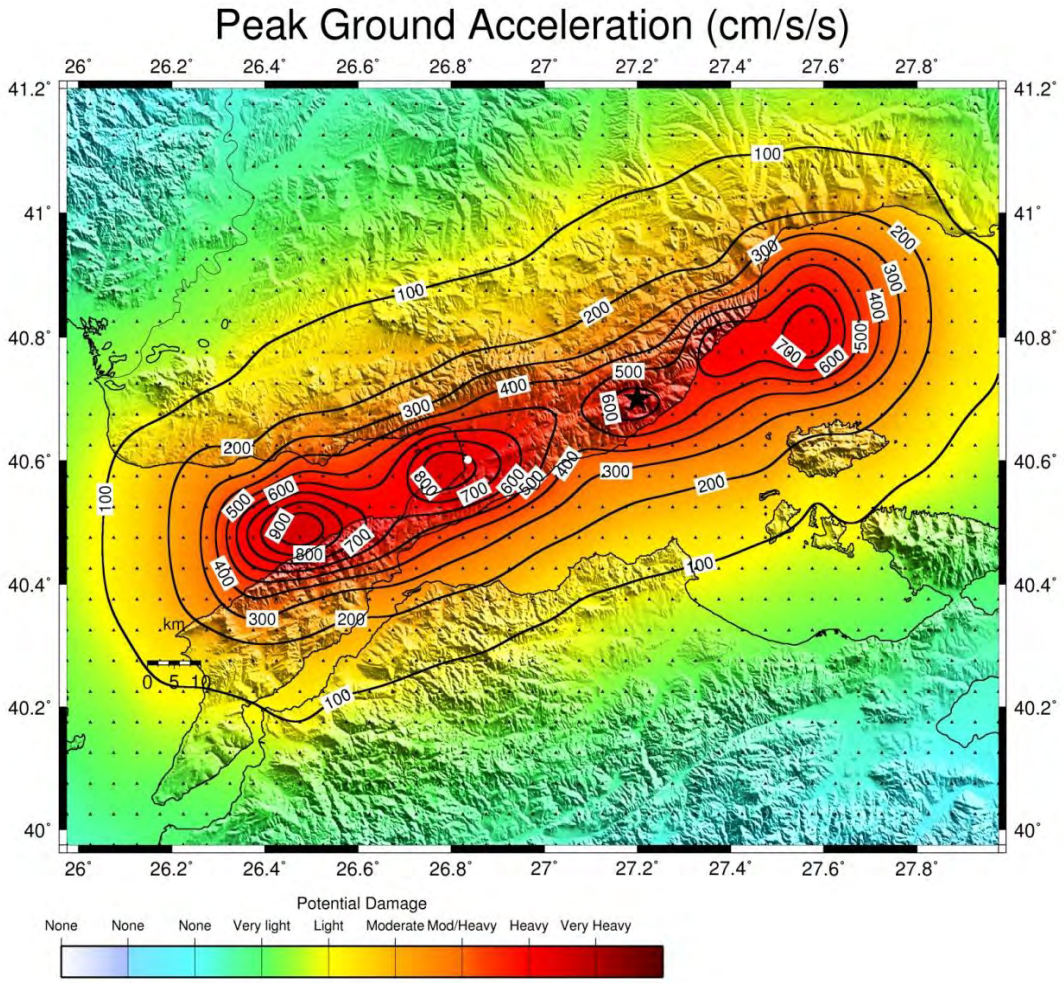

Figure 5 - Distribution of Peak Ground Acceleration at the broader region of the Ganos Fault, using stochastic simulations for a finite fault of length equal to 120 km and width of 18 km. The dots denote the grid nodes at which simulated acceleration time-histories were calculated, using the code of Beresnev and Atkinson (1998). The black star denotes the epicentre location.

Figure 6 provides the predicted level of intensities using the simulated accelerations at each node of the grid. It is observed that the mezoseismal region is well defined by the distribution of VIII to IX intensity level. For example the along major axis length of the area outlined by intensity 8 is approximately 120 km, as observed in the isoseismal maps of figure 2.

In conclusion, it is evident that to reproduce the gross characteristics of the distribution of damage of the 1912 Ganos earthquake a fault that extends both in Sea of Marmara as well as into the Saros Bay in the west, is required. In the simulations tested here, the results reproduce patches of strong shaking that are located at the ends of the fault, near Tekirdag in the east and north of Gelibolu in the west.

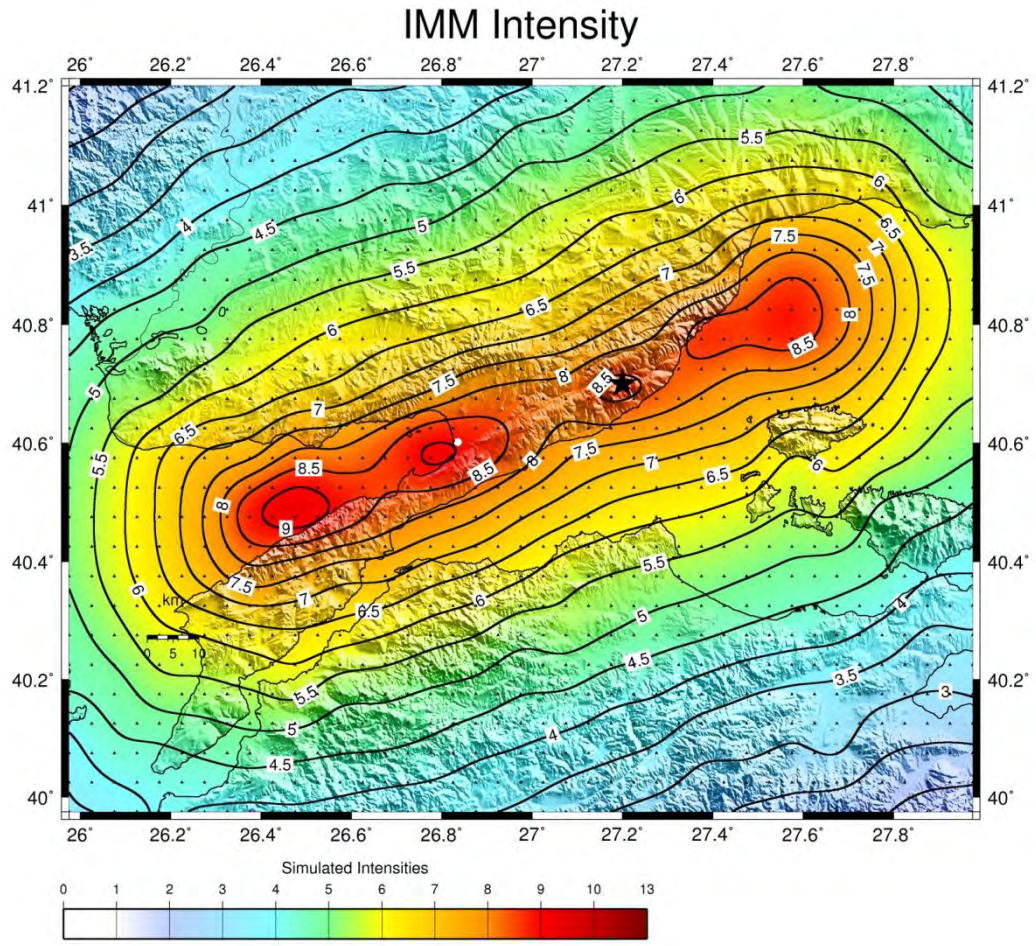

Figure 6 - ShakeMap for the 1912 Ganos mainshock, obtained from the simulated ground motions (PGA) at each node (dots) of the grid covering the broader region.

4. Conclusions

The 9 August 1912 Ganos fault earthquake (also known as Mürefte – Sarköy earthquake) together with the 1999 Izmit earthquake, are the two earthquakes which ruptured considerable part of the North Anatolian Fault, leaving its segments within the Marmara Sea un-ruptured. To this end, both events are significant mainly due to the imposed risk for the metropolitan city of Istanbul. The 9 August 1912 mainshock, Mw7.4, caused heavy damage, at the towns located along the Gaziköy – Saros segment of the North Anatolian Fault. It produced a well-mapped surface expression of the fault (Ambraseys and Finkel, 1987) along which slip measurements were performed (Altunel et al., 2004; Aksoy et al., 2010). The mainshock of August 9 was followed within hours by an Mw6.2 aftershock with an epicentre closer to the Marmara Sea. On 13 September 1912 another strong event occurred close to the Saros Bay, which is considered as a separate event rather as a late aftershock.

Even though most of the studies conclude that the focal mechanism of the 1912 earthquake is a N68°E dextral pure strike-slip fault (e.g. Aksoy et al., 2010), the length of the causative fault, is controversial. It is reported to be well above the 50km of the rupture mapped on land, and is considered to range between 90 and 150 km.

The purpose of this work was to test two end-members regarding the length of the causative fault. The method used was to stochastically simulate the level of strong ground motions, suing the approach of Beresnev and Atkisnson (1998) at a grid whose nodes cover the broader region. In one case the fault length is very conservative and is assumed to be only 50 km, and is placed on land exactly along the observed surface expression. In the other case, after many trials the fault length is chosen to be 120 km, which was found to better reproduce the observed pattern of damage. In both cases I examine the simulated PGA maps with respect to their ability to reproduce the gross characteristics of the observed surface faulting for the 1912 rupture.
In the first case, where a length of 50 km was used, that corresponds to the along –strike extent of the surface faulting the simulated ground motions can predict the areas of strong shaking but the area of strong shaking is considerably smaller than the one depicted within intensity VIII to IX in the observed isoseismal map. In the second case, where the fault length is taken 120 km, with 30 km extending in the Sea of Marmara, 50 km on land and 40 km in the Saros Bay, the simulated ground motion shaking better approximates the observed area of strong intensities as well as the regions where the measured slip exceeded 4 m (as reported in Aksoy et al., 2010). In both cases, the hypocenter was placed at the eastern end of the fault and the rupture initiation point was placed at the deeper part of the finite-fault. This means that the best results were obtained for unilateral rupture propagation from east towards west. As a result, the present study confirms the previous results for a fault length of approximately 120 km, as well as the fact that only a small segment within the western edge of the Sea of Marmara ruptured during the 1912 mainshock. The sea-bottom topography and the change of strike near Tekirdag, has affected the propagation of the rupture towards east.

5. Acknowledgments

This work was financed by **a)** the European Union (European Social Fund – ESF) and Greek national funds through the Operational Program "Education and Lifelong Learning" of the National Strategic Reference Framework (NSRF) - Research Funding Program: Thales “Investing in knowledge society through the European Social Fund and **b)** the General Secretariat for Research & Technology (GSRT) of Greece (Project Number: 10 TUR/1-3-52) in the framework of the Turkey-Greece bilateral project with title: “Turkey – Greece cross border seismicity: velocity models, moment tensors, slip models, shake maps based on knowledge- transfer and a joint database repository”. Figures were produced using the General Mapping Tools software (Wessel and Smith, 1998).

6. References

Aksoy E. M., Meghraoui M., Vallée M. and Cakir Z. 2009. Rupture Characteristics of the 1912 Mürefte (Ganos) Earthquake Segment of the North Anatolian Fault (Western Turkey), *Eos Trans. AGU 90(52)*, Fall Meet. Suppl., Abstract T13C-1884.

Altınok Y., Alpar B. and Yaltırak C. 2003. Şarköy- Mürefte 1912 earthquake’s tsunami, extension of the associated faulting in the Marmara Sea, Turkey, *Journal of Seismology*, 7, 329–346.

Altunel E., Meghraoui M., Akyuz S. and Dikbas A. 2004. Characteristics of the 1912 co-seismic rupture along the North Anatolian Fault Zone (Turkey): implications for the expected Marmara earthquake, *Terra Nova*, *16* (4), 198-204.

Ambraseys N.N. and Finkel C.F., 1987. The Saros-Marmara earthquake of 9 August 1912, *Earthquake Eng. and Struct. Dyn.,* 15, 189–211.

Ambraseys N.N. and Jackson J.A. 1998. Faulting associated with historical and recent earthquakes in the Eastern Mediterranean region, *Geophys. J. Int*., 133, 390–406.

Ambraseys N.N. and Jackson J.A. 2000. Seismicity of Sea of Marmara (Turkey) since 1500, *Geophys. J. Int*., 141, F1–F6.

Armijo R., Meyer B., Hubert A. and Barka A.A. 1999. Westward propagation of the North Anatolian fault into the northern Aegean: Timing and Kinematics, *Geology,* 27, 267–270.

Beresnev I. A. and Atkinson G. M. 1997. Modeling finite-fault radiation from the ωn spectrum, *Bull. Seism. Soc. Am.,* 87, 67 – 84.

Beresnev I. A. and Atkinson G. M. 1998. FINSIM – a FORTRAN program for simulating stochastic acceleration time histories from finite faults, *Seism. Res. Lett*., 69, 27 – 32.

Boore D. M. 1983. Stochastic simulation of high-frequency ground motions based on seismological models of the radiated spectra, *Bull. Seism. Soc. Am.,* 73, 1865 – 1894.

Borcherdt R. D. 1994. Estimates of site-dependent response spectra for design (methodology and justification), *Earthquake Spectra,* 10, 617- 653.

Shebalin N. and Karnik V. 1974. Catalogue of Earthquakes in the Balkan Region, UNESCO survey of seismicity of the Balkan Region, Part I, *Atlas of Isoseismal Maps*, Skopje, Yugoslavia.

Karabulut H., Roumelioti Z., Benetatos C., Ahu Komec M., Özalaybey S., Aktar M. and Kiratzi A. 2006. A source study of the 6 July 2003 (*M*w 5.7) earthquake sequence in the Gulf of Saros (northern Aegean Sea): Seismological evidence for the western continuation of the Ganos fault, *Tectonophysics*, 412, 195– 216.

Kiratzi A. and Louvari E. 2003. Focal mechanisms of shallow earthquakes in the Aegean Sea and the surrounding lands determined by waveform modelling: a new database, *Journal of Geodynamics,* 36 (1–2), 251–274.

Kiratzi A., Benetatos C. and Roumelioti Z. 2007. Distributed earthquake focal mechanisms in the Aegean Sea, *Bulletin of the Geological Society of Greece*, Vol. XXXX, 1125-1137.

Papadimitriou E.E., Karakostas V.G. and Papazachos, B.C. 2001. Rupture zones in the area of the 17.08.99 Izmit (NW Turkey) large earthquake (Mw 7.7) and stress changes caused by its generation, *J. Seismol.,* 5, 269–276.

Papazachos B. C. and Papazachou C. 2003. *The earthquakes of Greece*, Ziti Publ. Co., Thessaloniki, Greece, pp. 286 (in Greek).

Pulido N., Ojeda A., Atakan K. and Kubo T. 2004. Strong ground motion estimation in the Sea of Marmara region (Turkey) based on scenario earthquake, *Tectonophysics,* 39, 357-374.

Seeber L., Emre O., Cormier M.-H., Sorlien C. C., McHugh C. M. G., Polonia A., Ozer N. and Cağatay N. 2004. Uplift and subsidence from oblique slip: the Ganos–Marmara bend of the North Anatolian Transform, Western Turkey*, Tectonophysics,* 391, 239-258.

Wald D. J. and Allen T. I. 2007. Topographic slope as a proxy for seismic site conditions and amplification*, Bull. Seism. Soc. Am.,* 97(5), pp. 1379-1395.

Wells D. L. and Coppersmith K. J. 1994. New empirical relationships among magnitude, rupture length, rupture width, rupture area and surface displacement, *Bull. Seism. Soc. Am.,* 84, 974-1002.

Wessel P. and Smith W.H.F. 1998. New improved version of the Generic Mapping Tools released, *EOS Trans.* AGU, 79, 579.